LANGMUIR

pubs.acs.org/Langmuir Article

Cationic Imidazolium Polythiophenes: Effects of Imidazolium-Methylation on Solution Concentration-Driven Aggregation and Surface Free Energy of Films Processed from Solvents with Different Polarity

Sergio E. Domínguez,* Antti Vuolle, Michela Cangiotti, Alberto Fattori, Timo Ääritalo, Pia Damlin, M. Francesca Ottaviani, and Carita Kvarnström*

Cite This: *Langmuir* 2020, 36, 2278−2290 Read Online

ACCESS | Metrics & More | Article Recommendations | Supporting Information

ABSTRACT: Cationic imidazolium-functionalized polythiophenes with single- or double-methylation of the imidazolium ring were used to study the impact of imidazolium-methylation on (i) the solution concentration-driven aggregation in the presence of paramagnetic probes with different ionic and hydrophobic constituents and (ii) their surface free energy (SFE) as spin-coated films deposited on plasma-activated glass. Electron paramagnetic resonance spectroscopy shows that the differences in film structuration between the polymers with different methylations originate from the early stages of aggregation. In the solid state, higher degree of imidazolium-methylation generates smaller values of total SFE, γS, (by around 2 mN/m), which could be relevant in optoelectronic applications. Methylation also causes a decrease in the polar contribution of γS (γSp), suggesting that methylation decreases the polar nature of the imidazolium ring, probably due to the blocking of its H-bonding capabilities. The values of γS obtained in the present work are similar to the values obtained for doped films of neutral conjugated polymers, such as polyaniline, poly(3-hexylthiophene), and polypyrrole. However, imidazolium-polythiophenes generate films with a larger predominance of the dispersive component of γS (γSd), probably due to the motion restriction in the ionic functionalities in a conjugated polyelectrolyte, in comparison to regular dopants. The presence of 1,4-dioxane increases γSp, especially, in the polymer with larger imidazolium-methylation (and therefore unable to interact through H-bonding), probably by a decrease of the imidazolium−glass interactions. Singly-methylated imidazolium polythiophenes have been applied as electrode selective ("buffer") interlayers in conventional and inverted organic solar cells, improving their performance. However, clear structure−function guidelines are still needed for designing high-performance polythiophene-based interlayer materials. Therefore, the information reported in this work could be useful for such applications.

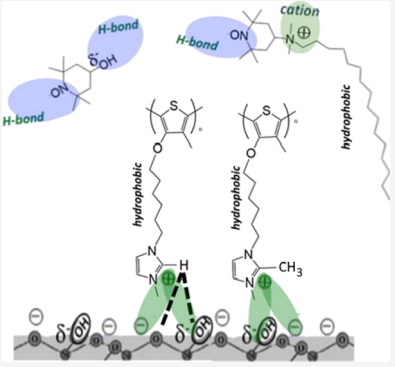

INTRODUCTION

Conjugated polyelectrolytes (CPEs) possess physical−chemical properties related to both "π" systems, like acting as chromophores and fluorophores, and properties of polyelectrolytes, such as solubility in high dielectric media (e.g., water and other polar solvents). They also possess the capability of coordination through electrostatic forces and hydrogen bonding (H-bonding) either with solvents, therefore helping in solubilization, or with other dissolved molecules.[1−3] The ionic groups in the polymers introduce ion−dipole and ion−ion forces.[4]

Furthermore, when CPEs contain functional groups with cationic π-rings (such as the heteroatomic imidazolium or pyridinium rings), the coaction between the noncovalent cation and π forces (also known as π^+) has to be taken into account. In recent years, $\pi^+-\pi$ and $\pi^+-\pi^+$ interactions have been recognized as a distinctive contributing factor in structuring in the context of host−guest chemistry and fundamental ab initio studies of $\pi-\pi$ interactions.[5] In ionic liquids (ILs) containing the imidazolium ring, dispersion and $\pi-\pi$ interactions also compete with hydrogen bonding (H-bonding), which in part determines the structuring in the IL.[5] When protonated, imidazoliums can establish H-bonds through their N−H group as it happens in the "doubly ionic" low-energy H-bonds present between histidine and aspartate during enzymatic catalysis.[6] According to qualitative molecular orbital computational analyses, methylation of the nitrogen atoms in imidazolium rings (known as aprotic imidazolium rings) does not cancel the H-bonding capabilities of the ring, which considers the cationic C−H group (C−H$^+$)

Received: October 4, 2019
Revised: January 13, 2020
Published: February 6, 2020

https://dx.doi.org/10.1021/acs.langmuir.9b03095
Langmuir 2020, 36, 2278−2290

to possess H-bonding donor capabilities.[7] This has also been considered in molecular dynamics simulations in order to explain the cooperative−competitive interplay between H-bonding and π-type interactions in an IL consisting of aprotic-imidazolium and oxalatoborate.[8]

Notice that because of the different definitions of H-bonding, in numerous studies, the classification of any interaction considered may be equivocal, as pointed in the review by Grabowski.[9] For example, numerous $C^+-H\cdots Y$ interactions have been classified as H-bonds; however, they could not be classified as such in the Pauling definition because carbon is not an electronegative atom.[9] In his review, Steiner pointed that despite the role of C−H groups as H-bond donors being underexplored, it could be predicted to occur when very acidic C−H group donors or very basic acceptor groups are involved.[6,10]

If present in CPEs, all of these forces are expected to impact their (i) solubility, (ii) conformation in solution, (iii) aggregation between polymer chains (intermolecular aggregation) and between different segments of the same chain (intramolecular aggregation), and (iv) interaction with other molecules either in solution (e.g. complex formation and assembly) or in solid state.

In the solid state, the solubility of CPEs is important in the fabrication of optoelectronic devices. For example, the use of water-soluble polythiophenes with ionic ammonium pendant groups allow orthogonal processing on top of the photoactive layer of organic solar cells (OSCs). This grants the formation of a capacitive double layer, enabling improved charge extraction and, thus, device efficiency.[11]

The power conversion efficiency of OSCs can be improved significantly by using electrode selective ("buffer") interlayers made of cationic or anionic CPEs, regardless of the ion functionality.[12] Such phenomena improve the efficiency of organic photovoltaics,[11−13] and therefore CPEs containing different ionic moieties are frequently used as electrode selective "buffer" layer materials.

Kelvin probe force microscopy (KPFM) or ultraviolet photoelectron spectroscopy (UPS) has been used to gain insight into the structure-function dependence and effect on the working mechanism of these buffer layers.[13] From these studies, different mechanisms have been proposed, such as (i) preferred orientation of the ionic moieties, (ii) energy level alignment at the organic/metal interface or active layer doping, (iii) formation of an image charge, causing alterations in the work functions,[13] or (iv) capability to show spontaneous permanent dipoles, poling-induced dipole alignment, and interfacial energy barrier control.[14,15]

Besides KPFM and UPS measurements, another approach is to characterize the photovoltaic properties of OSCs after including buffer layers made of CPEs, among other materials (e.g., LiF and Cs_2CO_3 of fullerene derivatives), affording remarkable improvements in conversion efficiencies.[16]

In the particular case of cationic polythiophenes used as buffer layers in a conventional OSC architecture (i.e., the bottom-metallic electrode act as the cathode, extracting electrons), Seo et al.[17] reported one of the first studies on improvement of OSCs by adding a cationic trimethylammonium polythiophene next to the metallic cathode. Later, Kesters et al.[16] compared the effect of applying cationic polythiophenes with either trimethylammonium or imidazolium side chains as buffer layers. The results showed that the presence of a cation−π system is desirable because the imidazolium functionality generates better device performance. In a subsequent study, the same group compared two polythiophenes containing either imidazolium or pyridinium side chains.[11,13] From their studies, it was concluded that a larger cation−π system is preferred, whereas the polymer having a pyridinium functionality performs better than that with an imidazolium group. With regard to the use of cationic polythiophenes in inverted architectures (i.e., with the metallic electrode acting as the anode by extracting holes), Zilberberg et al.[18,19] applied an ultrathin cathode buffer layer made of the same imidazolium polythiophene used by Kesters et al.[13,16] It was found that the buffer layer reduced the work function of the indium tin oxide (ITO) electrode (which under inverted architecture extracts electrons). In another work, Rider et al.[20,21] reported stable inverted OSCs fabricated using a cathodic buffer layer consisting of a mixture of a cationic pyridinium polythiophene and poly(3,4-ethylenedioxythiophene) polystyrene sulfonate.

Despite the mentioned studies, a clear mechanistic model to explain the working mechanism of buffer layers is not available yet. Therefore, clear structure-function guidelines are still needed for designing high-performance polythiophene-based interlayer materials.[11]

Contact angle (CA) goniometry is a useful route to gain insight into the properties of films of CPEs because it allows estimating the surface free energy (SFE or, simply, surface energy) of polymeric films. For example, in OSCs, increments in the total SFE (γS) of around 4 mN/m have been observed in poly(3-hexylthiophene) (P3HT) films because of a decrease in polymer regioregularity.[22] This was interpreted as a difference in the packing of the alkyl chains in P3HT, following previous studies on pentacene films, which showed (by means of CA goniometry) that a decreased film order increases γS (in less than 1 mN/m).[23] This result allowed explaining the high miscibility observed between P3HT and [6,6]-phenyl-C_{61}-butyric acid methyl ester $PC_{60}BM$[24] and later $PC_{70}BM$.[25] SFE also has an impact on the morphology, miscibility, and segregation between adjacent layers or between layers and electrodes in OSCs, in the end affecting the efficiency of the devices. For example, a difference of around 10 mN/m in γS between layers (29.1 and 41.1 mN/m) promotes poor miscibility, producing a slightly larger phase-separated film morphology.[22,25,26] However, when this difference decreases to around 2.5 mN/m (29.1 and 31.6 mN/m), penetration and diffusion of the fullerene into the polymer region are promoted.[11,22,25,26]

SFE analyses have been utilized to study the following: (i) the impact of CPE buffer layers on the short-circuit current and fill factor of OSCs,[27] (ii) the impact of surface treatments of buffers on the adhesion and power conversion efficiency of OSCs,[28] and (iii) the adhesive properties of the constituent layers in OSCs, which impact the mechanical stability of the device.[29]

The energy level, electrical conductivity, and SFE of films made of CPEs can be modified by means of molecular structure, for example, by changing the polymer backbone and the lengths of alkyl side chains.[15]

It is also possible to dope the films; for example, the archetypical P3HT generates films with a low surface energy. However, doped P3HT generates high surface energies mainly due to its conductivity, namely, the presence of radical cations and anions. The use of dopants with strong hydrophobic groups (e.g., tolyl groups), hydroxyl groups, and carboxyl

https://dx.doi.org/10.1021/acs.langmuir.9b03095
Langmuir 2020, 36, 2278−2290

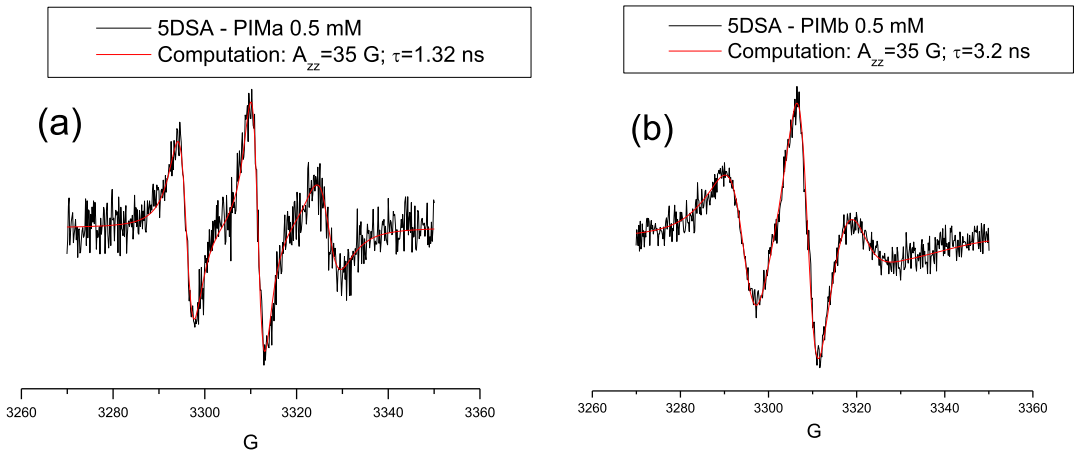

Figure 1. EPR spectra of the paramagnetic probe 5DSA in solutions of (a) PIMa and (b) PIMb at 25 °C and 0.5 mM.

groups also promotes intermolecular hydrogen bonds, modifying the wetting properties of the polymer. Polypyrrole (PPy) possesses Lewis acid−base contributions, predominately Lewis acidity. The most energetic part of the molecule is the acidic sites, possibly due to N−H bonds on the pyrrole acting as electron-pair acceptors (i.e., act as H-bonding donors) and/or the cationic nature of the backbone.[30]

Besides modifying the molecular structure of the polymer and/or doping the polymeric films, a judicious selection of the polarity of the solvent mixtures allows modulation of the nanomorphology of self-assembled aggregates (e.g., vesicles, rods etc.) as well as the optical properties of conjugated polymers and CPEs.[11] Cosolvents (also known as "additives" in the field of OSCs) provide an extra level of control over the main parameters that dominate the OSC formation during solution processing: (1) in solution, the thermodynamic parameters, such as the solubility of donor and acceptor materials in the solvent(s), their ability to undergo crystallization/aggregation, and the mutual interactions between the solvents and the donor and acceptor solutes and (2) the kinetic parameters, such as the vapor pressure of the solvents and the deposition conditions that collectively define the drying kinetics of the mixture.[31] CPEs are particularly tunable by means of solvents because these molecules allow the use of high dielectric media (e.g., water and hydroxylic solvents), offering a wider window of conditions and maximizing the possibility to study interaction forces. For the particular case of cationic imidazolium polythiophenes, Urbánek et al. have found that an imidazolium polythiophene shows solvatochromic concentration-driven aggregation, with methanol decreasing the extent of aggregation.[32] Our previous studies agree with this reference because we observed that a cationic isothiouronium polythiophene (which possess H-bonding donor capabilities) shows larger Stokes shifts when dissolved in water than when dissolved in mixtures with decreased polarity/H-bonding capacity, both in disaggregated[33] and aggregated[34] states.

This work presents a study on the effect of methylation of an imidazolium functionality in cationic polythiophenes. The focus is on their (i) concentration-driven aggregation in water and (ii) SFE of films processed from solvents with different polarities. The study of aggregation in aqueous media is studied by electron paramagnetic resonance (EPR) spectroscopy with the aid of paramagnetic probes of different polarities. The computer-aided analysis of the EPR spectra of polymers that are able to self-aggregate in aqueous solutions has demonstrated to be a useful tool to obtain information on the aggregation behavior and the interactions occurring in solution,[35,36] as shown in our previous study on the concentration-driven aggregation of cationic polythiophenes in water.[34] Therefore, EPR spectroscopy is an ideal complementary technique to further study the concentration-driven aggregation of imidazolium polythiophenes reported previously.[32]

The SFE was studied by CA goniometry measurements on spin-coated films of the polymers on plasma-activated microscope glass coverslips. The effect of the polarity and H-bonding capacity of the processing solvent was studied by using either water or a water−1,4-dioxane (DI) 50:50 (v/v) mixture (W−DI).

With regard to the imidazolium polythiophenes used here, the one with less extent of methylation is analogous to that used previously in studies in solution[32] or applied as buffer layers,[13,16,18] whereas that with methylation in the C^{+}−H group (see Figure 1b) has not been analyzed yet in such type of studies, to the best of our knowledge.

With regard to the solvents selected, DI is a nonpolar aprotic solvent with a boiling point and density similar to water, which also is miscible with water in all proportions. DI is also capable of disrupting the H-bonding structure in water by accepting two H-bonds, without donating any, because of its relatively bulky structure consisting of ether groups.[37] Besides this, the 50:50 v/v mixture of water and DI (W−DI), has a dielectric constant ≈50% smaller than that of water and a viscosity double that of water (see Table 1). Density functional theory studies have shown that complexation of molecules can be modulated by changing the amount of DI in water.[37] Molecular dynamics simulations of the interactions between the oligomers of an anionic phenylene−fluorene copolymer in water or the W−DI mixture showed that DI forms a "coating," displacing water from the immediate environment of the molecule, whereas the ionic parts are preferentially solvated by water. This coating reduces interchain and side-chain interactions and leads therefore to aggregation.[38] This coating effect is in agreement with the experimental study by Luong et al.,[39] who reported that heteromolecular water−DI H-bond dominates only at low concentrations of water, whereas at water mole fractions above 0.1, it generates a bulklike, intermolecular, three-dimensional H-bonded water network dynamics. Experimental studies of quenching in solution have

https://dx.doi.org/10.1021/acs.langmuir.9b03095
Langmuir 2020, 36, 2278−2290

Table 1. Values of Physical−Chemical Parameters Relevant for the Studies, from All Solvents (at 20 or 29 °C)[a]

solvent	density (g/cm^3)	dynamic viscosity (mPa s)	dielectric constant	refractive index
water	0.99[49]	[b]0.754[50]	80.38[51]	[b]1.33[50]
W−DI	1.03[52]	[b]1.4[50]	36.89[51]	[b]1.40[50]
solvent	H-bonding capacity[c]	δ_D dispersion[d]	δ_P polar[d]	δ_H hydrogen bonding[d]
water	strong	15.5	16.0	42.3
DI	moderate	17.5	1.8	9.0

[a]Also shown are the H-bonding capacities of each pure solvent (according to the Hildebrand scale) and the values of the H-bonding interactive force (δ_H) of the Hansen solubility parameters of each pure solvent. Next to each value is provided the reference number. [b]At 29 °C. [c]Ref 53. [d]Ref 54.

used the W−DI system because it provides a wide range of variation of solvent dielectric constant and viscosity, allowing to analyze their effects.[40]

Besides the computational and empirical studies in solution, with regard to studies focused on films, to the best of our knowledge, DI has been used as a cosolvent at very low concentrations (1−2%) when studying OSCs made of hydrophobic molecules.[41,42] It has not, however, been used in studies on thermodynamics in solution or drying kinetics of films using either hydrophobic or hydrophilic molecules.[31]

With regard to the glass substrates used, the polymeric films produced in this work can be considered as model surfaces similar to buffer layers in contact with oxide electrodes because both ITO[43,44] and plasma-activated glass[45] possess surface −OH groups. As mentioned before, in the context of OSCs, cationic imidazolium polythiophenes next to ITO substrates has been reported in devices with inverted architecture, in which the ITO electrode acts as the cathode, extracting holes.[18,20]

However, regardless of the surface properties of the substrate, the present work allows to study the effect of modifying the conjugated nature of the cationic functionality, as observed in the works of Kesters et al. cited before, having films of cationic polythiophenes next to aluminum substrates as a part of OSCs.[13,16]

Furthermore, the films obtained in this work allow comparisons with previously reported films made of neutral (nonionic) conjugated polymers, such as P3HT, polyaniline (PANI), and PPy, doped with different dopants (and also dedoped). These polymers showed similar ratios between the polar and dispersive contributions of the SFE, regardless of whether they were deposited onto glass or metallic (e.g., gold) substrates.[30]

MATERIALS AND METHODS

Unless otherwise stated, all reagents and solvents used are of analytical reagent grade, commercially available, and used as supplied (Sigma-Aldrich). Deionized water was used for the preparation of the stock solutions.

Scheme 1a shows the skeletal structure of the cationic imidazolium polythiophenes used in this work: poly-3-(1-methylimidazolium)-hexyloxy-4-methylthiophene (PIMa) and poly-3-(1,2-dimethylimidazolium)hexyloxy-4-methylthiophene (PIMb), whose self-assembling capacity has been previously described.[46]

These polymers are assumed to have mainly head-to-tail regioregularity because the syntheses were performed using 3-alkoxy-4-methylthiophene monomers in an oxidative polymerization (using $FeCl_3$), conditions that are known to generate mainly 2,5

Scheme 1. Skeletal Structures of (a) the Cationic Imidazolium Polythiophenes PIMa and PIMb and (b) the Paramagnetic Probes Used in the EPR Aqueous Study, TOH, CAT8, CAT16, and 5DSA

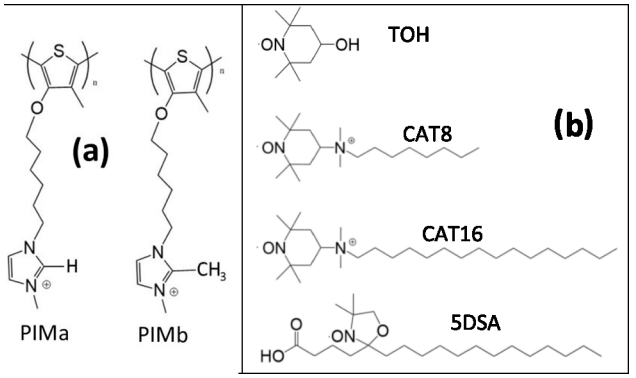

linkages.[47] The polymers are also assumed to have a similar degree of polymerization (20−30 repeating units) and dispersity ($Đ = M_w/M_n$ = 1−3). For further details on these assumptions, please see ref 33.

Scheme 1b shows the structures of the paramagnetic spin probes used in this work. 4-hydroxy-2,2,6,6-tetramethyl-piperidine-1-oxyl (TOH) and 5-doxyl-stearic acid (5DSA) are commercially available, and 4-octyl dimethyl ammonium, 2,2,6,6 tetramethyl-piperidine-1-oxyl bromide (CAT8) and 4-cetyl dimethylammonium, 2,2,6,6 tetramethyl-piperidine-1-oxyl bromide (CAT16) are a gift from Dr. Xuegong Lei, Columbia University, NY, USA. These probes were selected after accurate screening and found to be the most suitable to get information about the formation of aggregates and about the interacting ability of PIMa and PIMb in water because they were previously demonstrated to be informative on the structure and aggregation of polymers and surfactants.[35,36] These spin probes have also been used in our previous EPR study on the concentration-driven aggregation of cationic polythiophenes.[34]

EPR Spectroscopy. EPR spectra were recorded by an EMX-Bruker spectrometer operating at X band (9.5 GHz) and interfaced with a PC (software from Bruker for handling and recording the EPR spectra). The temperature was controlled by a Bruker ST3000 variable temperature assembly cooled with liquid nitrogen. The reproducibility was verified by repeating each experiment at least three times.

The concentration of 0.05 mM was selected for all probes because it showed to be nonperturbative of the systems on the basis of the invariability of the spectral line shape by further decreasing this concentration.

The computation of the spectra was accomplished by means of the well-established procedure of Budil et al.[48] The EPR spectral line shape is determined by the molecular reorientational dynamics of the spin probe and its constraints over correlation times ranging from 10^{-11} to 10^{-6} s. According to the Kubo−Tomita theory, it is possible to simulate EPR spectra on the basis of peculiar dynamic models.[48] Anisotropies of the reorientational motion of anisotropic molecules, for example,, nitroxide molecules, mainly surfactants, were accounted for by introducing simple potentials. A modification of the Levenberg−Marquardt minimization algorithm was used for the analysis of the EPR spectra. The dynamic parameters describing the slow motion are obtained from the least-squares fitting of model calculations based on the stochastic Liouville equation of the experimental spectra. The correlation time obtained provides a measure of microviscosity at the nitroxide site.

The main parameters extracted from computation were the following: (i) the A_{ii} components of the hyperfine coupling tensor **A** for the coupling between the electron spin and the nitrogen nuclear spin. These components measure the environmental polarity. Unless otherwise specified, for simplicity, the A_{xx} and A_{yy} components were assumed to be constant (6 G), whereas only A_{zz} was changed. The

https://dx.doi.org/10.1021/acs.langmuir.9b03095
Langmuir 2020, 36, 2278−2290

accuracy of this parameter is ±0.01 G; (ii) the correlation time for the diffusional rotation motion of the probe (τ), which measures the microviscosity around the probe, in turn monitoring the interactions occurring among the molecules at the probe site. The accuracy in this parameter is ±1 ps.[35]

The total intensity of well-reproducible EPR spectra was evaluated by the double integral of the spectra in arbitrary units (A.U.). Quantitative EPR measurements of spin concentration cannot be performed in the absence of an internal reference, but, in the present case, we trusted the intensity values only in a comparative way for a series of samples for an indirect measure of the spin-probe solubility.

Solvent Systems. Table 1 shows some relevant physical−chemical properties of water and W−DI.

Spin-Coating Preparation of Glass Blanks and Polymeric Films. Spin-coated films of PIMa and PIMb were deposited either from water or W−DI on air-plasma-cleaned microscope borosilicate glass coverslips (VWR International). Air-plasma decreases the number of siloxane groups while increasing the surface concentration of H-bonding donor OH groups[55] and thus increasing the value of the "silanol number."[56] Besides the polymers, the plasma-activated glass slips were spin-coated only with water or DI in order to obtain the "glass−water" and "glass−DI" blanks, respectively.

The polymeric films were produced by adding 3 μL of 0.2 mg/mL solutions of PIMa or PIMb (for concentrations ≈ 0.8 mM, monomer based) dissolved either in water or W−DI on an already 500 rpm spinning substrate (i.e., dynamic dispense). Previously, a PIMa concentration of 0.25 mg/mL in water was used in this group to produce self-assembled multilayers of CPEs.[46] Also, in the previously mentioned studies of Kesters et al. using cationic polythiophenes, concentrations ≤ 0.25 mg/mL (in methanol) showed to be optimal to observe differences in OSC efficiencies as a function of the cationic functionality in the polythiophene.[13]

Despite these references, we analyzed the effect of increasing the surface concentration by using multiple depositions (with a drying of 60 s between each) using different cationic polythiophenes. Larger surface concentrations did not increase the difference between polymers (results not shown).

All solutions were obtained from the same aqueous stock solution (2.1 mM). The polymers are expected to interact with the plasma glass through electrostatic interactions between the cationic imidazolium units and the partial negatively charged surface −OH groups.

In order to maximize reproducibility (i.e., decrease the experimental error), all films were produced from the same batch solutions and by the same operator. In order to minimize the biased data due to the learning curve of the process, the production of films and the CA measurements were randomized as much as possible by avoiding to systematically produce or measure films exposed to the same treatment (i.e., same polymer or processing solvent) or similar measurements (e.g., same probe liquids).

Expected Interactions with Plasma-Glass. Scheme 2 shows the expected interactions between the plasma-activated glass substrates and the polymers.

CA Goniometry and SFE Estimations. CA measurements allow estimating the SFE of films made of conducting polymers in a relatively simple way (when compared with other techniques such as inverse gas chromatography), however, providing high sensitivity.[30] The CA between a liquid and a surface of interest can be related to the surface tension or energy via Young's equation together with different models (details ahead).[30] If CA values with two or more test (or "probe") liquids, with known and convenient surface tension components, are available, then it is possible to estimate the total free energy and also its Liftshitz−van der Waals (dispersive) and Lewis acid−base (polar) components.[30]

The estimations of the total SFE (γS), together with their polar (γSp) and dispersive (γSd) contributions, of the substrate blanks and polymer films were obtained using two models: the Owens, Wendt, Rabel, and Kaelble (OWRK) model and the Wu model (also known as the harmonic mean method).[60] Both methods have been described elsewhere,[61] and it is known that they require less measuring data than other models for estimation of γS, γSp, and γSd while avoiding generating negative values as other methods (e.g., the acid−base method).[61] Wu's model has already been used to study films made of conjugated polymeric molecules.[30,62−64]

Scheme 2. Expected Interactions between the Imidazolium CPEs Used in This Work and the Plasma-Activated Glass, Modified from Refs 57−59; Notice That the Glass Substrate Here Is Presented as Partially Activated, i.e., with a Partial Surface Concentration of Si−OH Having Also Si−O−Si Groups

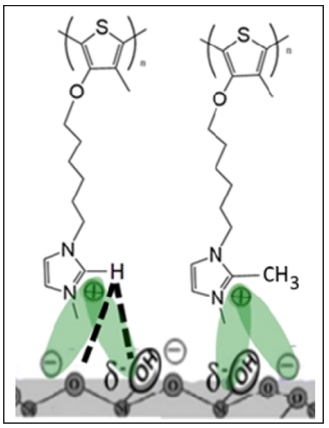

The SFE estimations by Wu's method were obtained considering the four probe liquids shown in Table 2 (glycerol, ethylene glycol, formamide, and diiodomethane), whereas the OWRK estimations were obtained considering two probe liquids (glycerol and diiodomethane).[61]

Table 2. Total Surface Tension (γL) of the Probe Liquids Used in This Work Together with Their Constituting Dispersive (γLd) and Polar (γLp) Contributions

	glycerol	ethylene glycol	formamide	diiodomethane
γL (mN/m)	63.4	47.7	58.2	50.8
γLd (mN/m)	37	26.4	39.5	48.5
γLp (mN/m)	26.4	21.3	18.7	2.3

The calculations to estimate the SFE were performed with the aid of the software KSV Surface Free Energy Analysis (version 3.0), copyright KSV Instruments, Ltd. (1997−2005), using the averages of at least triplicate CA measurements from different experimental units.

In this work, the CAs between the blank surface or polymeric films and different probe liquids (glycerol, ethylene glycol, formamide, and diiodomethane) were measured using the sessile drop method, with 3 μL drops of each probe liquid. The CA value was taken from the stabilized reading. The surface tension values of the respective liquids (γL) and their constituting polar and dispersive forces (γLp and γLd, respectively) are shown in Table 2.

Notice that the surface tension of liquids and SFE of solids are commonly reported in the literature either with units of force/unit length (mN/m) or energy/unit area (mJ/m^2), with both scales being numerically equivalent.

RESULTS AND DISCUSSION

EPR. EPR spectroscopy was successfully applied to investigate the aggregation mechanism of the differently methylated polymers described above. Characterization of the interaction between EPR probes and the polymer system is given by the interpretation of the experimental data by the use of the computer aided analysis described in the experimental section. The completely hydrophobic probe (5DSA) generated

https://dx.doi.org/10.1021/acs.langmuir.9b03095
Langmuir 2020, 36, 2278−2290

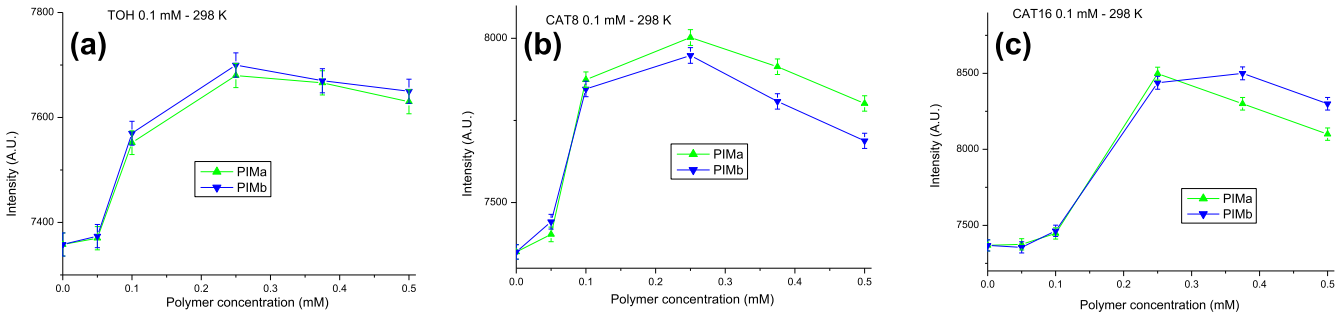

Figure 2. EPR spectral intensity (measured as a double integral of the spectra in A.U.) as a function of the concentration of PIMa (green upward triangles) and PIMb (blue downward triangles) in the presence of 0.1 mM TOH (a), CAT8 (b), and CAT16 (c).

different results with respect to probes containing hydrophilic and hydrophobic groups (TOH, CAT8, and CAT16). Therefore, the results obtained with 5DSA will be discussed separately.

Figure 1 shows the spectra recorded for 5DSA with (a) PIMa and (b) PIMb at 0.5 mM.

The spectra shown in the figure were recorded under the same experimental conditions as used for the other spin probes, for a matter of comparison. These spectra are quite noisy, demonstrating the low intensity due to the low solubility of 5DSA in these systems because it only solubilizes into the hydrophobic region formed by polymer aggregates. However, we clearly see that the noise is lower for PIMb than for PIMa, indicating higher solubilization of the hydrophobic probe in PIMb aggregates because of methylation of the imidazolium ring, which increases hydrophobicity.

The computations of the spectra (red lines; the main parameters A_{zz} and τ are listed in the figure) interestingly indicate that the radical group (at position 5 of the stearic chain) is located in a region at low polarity and quite high microviscosity, as expected for the hydrophobic core of a lipid aggregate. A significantly higher microviscosity (more than the double) was calculated for PIMb with respect to PIMa, indicating that methylation of the imidazolium function increases the microviscosity in the environment of the hydrophobic probe inserted into the polymer aggregates.

Effect of Imidazolium Methylation on the EPR Intensity. With regard to the results from the probes TOH, CAT8, and CAT16, Figure 2 shows the intensity variation (measured as a double integral of the spectra) as a function of the polymer concentration (in the 0−0.5 mM polymer concentration range) for TOH (a), CAT8 (b), and CAT16 (c).

Figure 2 shows that for all paramagnetic probes, a maximum intensity is observed at about 0.25 mM of polymer concentration. Assuming that the intensity measures the probe solubility, this result indicates increased probe solubility around this concentration. All probes contain a hydrophilic and hydrophobic portion and solubilize better when they insert in aggregates where the hydrophobic part is protected from the hydrophilic one. Therefore, we may consider the intensity increase as a proof of the formation of polymer aggregates, where the hydrophobic parts of the polymers condense surrounded by the hydrophilic parts. A previous study from our group using steady-state fluorescence on solutions of cationic isothiouronium polythiophenes also showed aggregation of the polymers around a polymer concentration of 0.2 mM.[34]

The equivalent solubilization of TOH in the aggregates of PIMa and PIMb shown in Figure 2a is reasonable because TOH is the most hydrophilic probe and therefore interacts with the cationic imidazolium groups regardless of their degree of methylation.

The fact that both polymers interact to a similar extent with TOH, despite the difference in the H-bonding capabilities between them, can be explained because water (and other hydroxylic solvents) is known to compete for intermolecular H-bonding; this is why they are known as "competitive solvents" in the contexts of molecular recognition[65,66] or polymer solvation.[67] Therefore, in this case, water would compete with TOH for the H-bonding, nulling the structural difference between PIMa and PIMb with regard to their H-bonding capabilities.

On the other hand, Figure 2b shows that for polymer concentrations associated with aggregation of cationic polythiophenes,[33,34] CAT8 generates larger intensities in the presence of the polymer with less extent of methylation in the imidazolium ring (PIMa). This is because this probe solubilizes at the hydrophilic/hydrophobic interface of the aggregates, and the methyl groups partially impede solubilization.

Interestingly, Figure 2c shows that, for a probe with a larger hydrophobic nature (CAT16), larger intensities are obtained in the presence of the polymer with larger extent of methylation in the imidazolium ring (PIMb). In this case, the methyl groups favor the solubilization in the disordered aggregates of the CAT16 probe whose hydrophobic portion has good affinity for hydrophobic methyl groups.

Figure 2b,c shows that, when interacting with CAT8 and CAT16, the highest polymer concentrations cause the curves of PIMa and PIMb to diverge. This behavior is opposite to that observed during the concentration-driven aggregation of isothiouronium polythiophenes with spacers of different lengths, under identical experimental conditions to the present work.[34]

In the previous study, the intensity increase to the maximum and, then, the decrease at the highest concentration have been ascribed to the formation of aggregates at the maximum, which became progressively less organized with the further increase in the concentration. For the isothiouronium polythiophenes, the longer spacer provokes the formation of better organized aggregates at the maximum, whereas the highest concentration of polymers equivalently leads to disorganization of the aggregates for the two polymers, despite the spacer length. In the present case, the methyl group is not perturbing the aggregate formation at the maximum, but only a high concentration of the polymer lets the methyl group differently affect the disorganizing process. This is because the methyl

https://dx.doi.org/10.1021/acs.langmuir.9b03095
Langmuir 2020, 36, 2278−2290

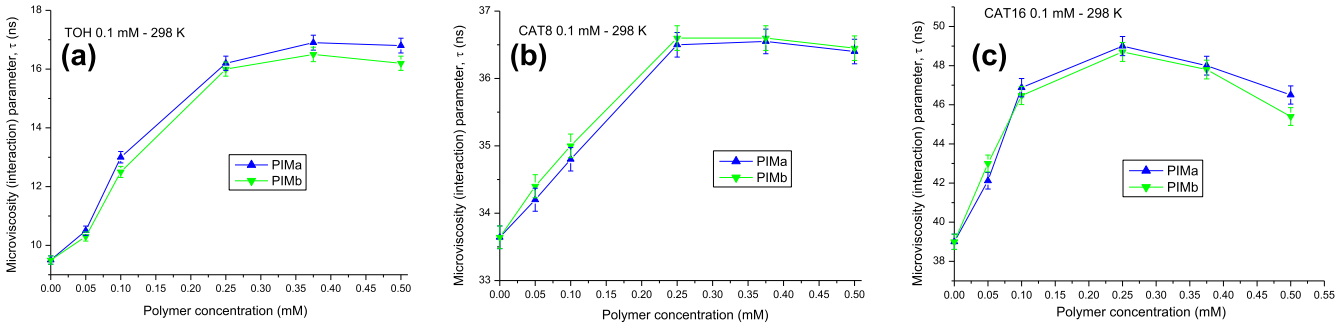

Figure 3. Microviscosity (interaction) parameter (τ) as a function of the concentration of PIMa (blue upward triangles) and PIMb (green downward triangles) in the presence of 0.1 mM TOH (a), CAT8 (b), and CAT16 (c).

Table 3. CA Values of the Four Probe Liquids onto (i) Plasma-Activated Glass, (ii) Plasma-Glass Spin-Coated with Water (Glass−Water), and (iii) Plasma-Glass Spin-Coated with DI (Glass−DI)

	blank surface		
probe liquid	plasma glass CA (deg) ± SD[a]	glass−water CA (deg) ± SD[a]	glass−DI CA (deg) ± SD[a]
glycerol	37.55 ± 7.35	39.39 ± 6.6	44.44 ± 5.39
ethylene glycol	21.87 ± 5.14	24 ± 5.82	30.05 ± 2.76
formamide	7.23 ± 1.94	14.4 ± 1.57	16.76 ± 1.87
diiodomethane	38.46 ± 3.86	43.22 ± 3.71	43.35 ± 2.66

[a]SD values based on at least triplicate (see Table S1 in the Supporting Information).

Table 4. SFE and Its Components Estimated from Films Processed from Water and the W−DI Mixture According to OWRK Model (Estimated Using Data from Glycerol and Diiodomethane) and Wu's Model (Estimated Using Data from the Four Probe Liquids)

		SFE					
	surface	OWRK γS (mN/m)	OWRK γSp (mN/m)	OWRK γSd (mN/m)	Wu γS (mN/m)	Wu γSp (mN/m)	Wu γSd (mN/m)
blank	plasma-glass	54.13	13.76	40.38	54.89	13.64	41.25
	glass−water	52.39	14.43	37.95	53.16	14.1	39.06
	glass−DI	49.86	11.98	37.89	51.78	12.44	39.34
PIMs	PIMa from water	58.79	13.95	44.84	57.72	13.28	44.45
	PIMa from W−DI	58.9	15.46	43.44	57.52	14.2	43.32
	PIMb from water	56.37	11.98	44.39	55.84	11.43	44.4
	PIMb from W−DI	54.25	10.43	42.81	55.43	12.33	43.10

group is located at the charged head and starts being perturbative only when the concentration of polymers is high and the charged head groups start repulsing each other.

Effect of Imidazolium-Methylation on Microviscosity. Figure 3 shows the microviscosity (interaction) parameter (τ) as a function of the concentration of PIMa and PIMb (also in the 0−0.5 mM polymer concentration range) for TOH (a), CAT8 (b), and CAT16 (c).

In Figure 3, it is observed that the differences between PIMa and PIMb at high concentrations are small (e.g., in Figure 3a,c); however, these differences are above the experimental error and in agreement with the other results. Figure 3a,c shows that the more hydrophilic and more hydrophobic probes, respectively, indicate a larger viscosity in the aggregates of the polymer with less extent of methylation in the imidazolium ring. Interestingly, Figure 3b shows that the probe with a middle extent of hydrophilic and hydrophobic components (compared with TOH and CAT16) indicates the same viscosity, regardless of the polymer. As suggested on the basis of the intensity data, the positively charged CAT group of CAT8 is hosted at the hydrophilic/hydrophobic interface, and it is repulsed by the positively charged polymer head. Therefore, the interactions do not feel the presence of the methyl groups. Conversely, both the neutral probe (TOH) and the largely hydrophobic probe CAT16 feel the presence of the methyl groups in the aggregates, which perturb the hydrophilic interactions at the highest PIMb concentrations, thus decreasing the microviscosity.

To better understand the intensity and microviscosity variations and the consequent information on the system structures, it is interesting to compare the behavior of two more hydrophobic probes, 5DSA and CAT16, with respect to the two polymers. Both probes show higher solubilization in PIMb aggregates because of methylation and increased hydrophobicity. However, the microviscosity for the methylated-PIMb sample, compared to PIMa, increases for 5DSA, whereas it decreases for CAT16. The radical group of 5DSA is at position 5 of the carbon chain, and hence it is embedded into the hydrophobic portion of the aggregates in proximity to the interface. Therefore, PIMb aggregates are more packed in their hydrophobic region than PIMa aggregates because of the presence of the methyl group in PIMb, which is thus located in the lipidic region where the doxyl group of 5DSA is situated, close to the interface, and increases the PIMb aggregate packing. Conversely, the radical CAT group of CAT16 is positively charged and stays outside the lipidic region. The

https://dx.doi.org/10.1021/acs.langmuir.9b03095
Langmuir 2020, 36, 2278−2290

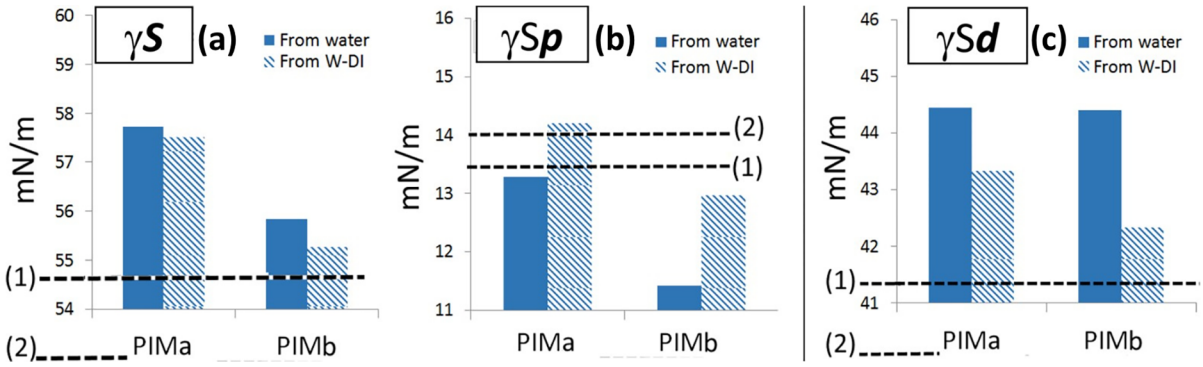

Figure 4. Wu's model estimations of (a) γS and its (b) polar component (γSp) and (c) dispersive component (γSd) of films made of PIMa and PIMb, processed from water (solid color bars) or W−DI (dash-patterned bars). Dashed horizontal lines indicate the SFE, SFEp, and SFEd values of the blank surfaces of (1) plasma glass and (2) glass−water.

long C16 chain forces this probe to solubilize in the PIMb aggregates (while CAT8 can escape!). However, by itself, the CAT group of CAT16 is also forced to approach the positively charged imidazolium group. Therefore, charge repulsion provokes the weakening of hydrophilic interactions and the consequent decrease in microviscosity.

CA Goniometry and SFE. Table 3 shows the average CA values of each of the four probe liquids on three blank surfaces: (i) plasma-activated glass (plasma glass), (ii) plasma glass spin-coated with water (glass−water), and (iii) plasma glass spin-coated with DI (glass−DI). Table 4 shows the OWRK and Wu estimations of the total SFE (γS) in the three blank surfaces and in the films of PIMa and PIMb on plasma glass. The values of the polar (γSp) and dispersive (γSd) contributions are also shown.

The data presented in Table 4 shows that OWRK and Wu models do not generate the same values of γS, γSp, and γSd. In the case of PIMa, Wu's model estimates smaller values than OWRK, regardless of the processing solvent. In the case of PIMb, when processed from water, the OWRK model estimates larger SFE values, whereas when processed from W−DI, the Wu's model estimates a larger value of SFE.

Regardless, both models generate the same trends with regard to the effect of the molecular structure and the processing solvent. Therefore, for the sake of simplicity and also to allow comparing with previous reports (all references cited ahead used Wu's model), Figure 4 shows only the SFE values estimated with Wu's model for blank surfaces and polymeric films.

CA Values of Blanks. The average CA of formamide on the glass−water blank (14.4°, Table 2) is 40% smaller than that reported by Rymuszka et al. of formamide on glass previously exposed to water during ultrasonic cleaning and drying (≈25°).[68] However, the average CA from diiodomethane on glass−water blank (43°) is similar to that of diiodomethane reported in the same reference (≈45°). Concerning the SFE values of the blanks, Table 4 shows that both models estimate similar total SFE values of the glass−water blank (≈53 mN/m). This value is 15% smaller than that estimated for nonheated glass with controlled porosity reported by Jańczuk et al. (≈70 mN/m).[69]

With regard to the CA values, the difference between the cited reference and our data could be due to (i) a possible difference in the type of glass, for example, soda lime glass instead of borosilicate, which are known to have different smoothness, see ref 70, and/or (ii) the difference in the drying conditions after exposure to water. These factors, alone or combined, would generate a different hydration in each glass. Because of the hydrophilic interactions of water, such a difference in hydration is expected to be clearer when using a polar probe liquid and less clear when reducing the polarity of the probe liquid. This is in agreement with the fact that the CA and SFE results obtained in the present work are similar to those of diiodomethane in the work of Rymuszka et al.[68] and SFE estimations of Jańczuk et al.,[69] respectively.

Given the experimental design of the present work, the glass−water blanks are useful regardless of previous reports; however, the references cited show that our results lie within the range of previously reported values.

SFE of Polymeric Films and Blanks and Previously Reported Values. Figure 4a shows that, from both the processing solvents, the films of PIMa have larger values of γS (by at least 2 mN/m) than those of any of the blanks. The films of PIMb also generate larger values of γS than the blanks, albeit in a smaller range. With regard to the components of γS in the polymeric films, Figure 4b shows that γSp of the glass−water blank is larger than those of the polymeric films (with the exception of the PIMa films processed from W−DI).

This indicates that, with the exception of the PIMa films processed from W−DI, the surface concentration and/or energy of imidazolium cationic units in the films are smaller than those of the −OH groups present in the glass−water blank. Thus, the PIMa films processed from W−DI would have a similar surface concentration of ionic groups (imidazolium and/or −OH).

Figure 4b also shows that the polymer with larger imidazolium ring methylation (PIMb) has smaller γSp than PIMa. This indicates that the alkylation impacts the polarity of the film. On the other hand, Figure 4c shows that, for both polymers, the γSd component is always larger than that in any of the blanks, regardless of the processing solvent, which gives evidence of the presence of the hydrophobic components in the polymers (i.e., thiophene rings and alkoxy spacer) on the glass substrate.

Effect of Imidazolium-Methylation on the SFE. Figure 4a shows that regardless of the processing solvent, the PIMa films have a larger γS (≈57 mN/m) than the PIMb films (≈55−56 mN/m). This decreased imidazolium-methylation increases γS. In this regard, a previous study on the effect of the regioregularity of P3HT on its surface energy as films showed that decreased packing of alkyl chains (due to smaller regioregularity) increases $\gamma S \approx 4$ mN/m.[22] Such a conclusion

https://dx.doi.org/10.1021/acs.langmuir.9b03095
Langmuir 2020, 36, 2278−2290

was made after studies on pentacene films, which showed (by means of CA goniometry) that a decreased film order increases γS (in less than 1 mN/m).[23] Therefore, our results suggest that the smaller extent of imidazolium-methylation in PIMb decreases film ordering, thereby decreasing γS.

The magnitude of the change in γS because of methylation could be useful when tuning the morphology, miscibility, and segregation between adjacent layers or between layers and electrodes in applications such as OSCs. In such devices, a difference of around 10 mN/m in γS between two layers (having 29.1 and 41.1 mN/m) promote poor miscibility, generating a larger phase-separated film morphology. However, when this difference decreases to around 2.5 mN/m (29.1 and 31.6 mN/m), penetration and diffusion of the fullerene into the polymer region are promoted.[11,22,25,26]

With regard to similarities with previously reported films of neutral conjugated polymers, PIMa films show γS values similar to those of HCl-doped films of PANI (57.9 mN/m), whereas the PIMb films show values similar to those reported from doped P3HT films on glass (54 mN/m) and $FeCl_3$-doped PPy films (55.4 mN/m). Notice that, as in the review by Higgins and Wallace,[30] these similarities have only a qualitative nature because the references cited were obtained using different methods and substrates. However, though qualitatively, these previous reports of neutral conjugated polymers allow analyzing the effects of regular- and "self"-doping present in neutral conjugated polymers and CPEs, respectively.

The γSp and γSd contributions provide further information. For the case of γSp, Figure 4b shows that regardless of the processing solvent, PIMa has larger values of γSp (by around 1.5 mN/m) than PIMb. As mentioned before, differences of around 2 mN/m are relevant when it comes to the SFE of films of conjugated polymers.[22,25,26]

In the case of γSd, when processed from W−DI, PIMa has a larger value of γSd (by around 1 mN/m) than PIMb.

In the case of films processed from water, the difference in γSp between polymers is negligible. In this case, PIMa and PIMb have γSd values of 44.45 and 44.4 mN/m, respectively.

In resume, from both processing solvents, imidazolium-methylation causes a clear decrease only in the case of γSp. This suggests that the imidazolium-methylation has an impact mainly on the polar component of the SFE. This could be related to a decrease of the π-enhanced cationic nature of the imidazolium functionality caused by methylation.

It is beneficial to use the ratio between the dispersive and polar contributions ($\gamma Sd/\gamma Sp$), because the relative contribution of the γSp and γSd components provides information about the structural differences of the films produced using CPEs and those produced from neutral CPs, doped or dedoped.

PIMa films generate $\gamma Sd/\gamma Sp$ ratios of ≈3.3 and ≈3 when processed from water or W−DI, respectively. These values are at least 33% larger than those reported in films of HCl-doped PANI on glass ($\gamma Sd/\gamma Sp \approx 2$).[30]

On the other hand, PIMb films generate values of ≈3.9 and ≈3.3 when processed from water and W−DI, respectively. These values are at least 60% larger than those reported in doped films of P3HT on glass or PPy on polyethylene terephthalate, which generate $\gamma Sd/\gamma Sp$ ratios of 1.42 and 2, respectively.[30,63]

The PIMa and PIMb films have similar γS values of previously reported doped-P3HT or PPy films, respectively, but the similarity does not hold concerning the value of the ratios $\gamma Sd/\gamma Sp$: the PIMa-PIMb films have larger $\gamma Sd/\gamma Sp$ than these references. In fact, the $\gamma Sd/\gamma Sp$ ratio of the PIMa−PIMb films (ranging in values of 3−4) are similar to those of dedoped films of P3HT and PPY, which have ratios of 4.14 and 2.63, respectively.[30,63]

These results indicate that the cationic functionalities in CPEs do not contribute to the polar nature of the films as much as regular dopants do. This could be related to the fact of the freedom of mobility that regular dopants have, in comparison with the restricted nature of the cationic functionalities attached to a CPE.

Effect of the Processing Solvent on the SFE. The components of the SFE (Table 4 and Figure 4b) show that the presence of DI increases the value of γSp: for PIMa and PIMb films, these increases are 7 and 13%, respectively. On the other hand, Figure 4c shows that DI decreases γSd in a similar extent for both polymers (for PIMa and PIMb films, these decreases are of 3 and 5%, respectively).

To further analyze the causes behind the increase in γSp due to the presence of DI, it is useful to use the CA data from the most nonpolar probe liquid, following the contribution by Tsai et al.[64] These authors studied a film of PPy, electropolymerized in the presence of dodecylbenzenesulfonate (DBS), on top of Si coated with Au/Cr. Then, the PPy in the film was electrochemically reduced or oxidized in an aqueous solution using sodium nitrate as the electrolyte while measuring in situ the CA values of dichloromethane, the least probe liquid tested.

Electrochemical reduction caused larger dichloromethane CA values, indicating a larger surface concentration of ionic sulphonate groups (from DBS).Contrarily, the oxidized state of the film caused smaller CA values, indicating a larger surface concentration of the dodecyl chain in DBS.

Thus, Table S1 shows that the CA values of diiodomethane on PIMa films processed from water is 28.5 ± 2.45°. This value is ≈3° smaller than that on films processed from W−DI (31.85 ± 6.2°). In the case of PIMb films, the effect of W−DI is larger: the CA values of diiodomethane on films processed from water (29.59 ± 0.48°) is also ≈3° smaller than those on films processed from W−DI (32.94 ± 2.6°).

These results suggest that, in the same extent for both polymers, the presence of DI in the processing solvent generates films with larger surface concentration of ionic imidazolium groups, which generate larger CA values with the most nonpolar probe liquid diiodomethane. Considering these results, a possible mechanistic explanation would be that DI decreases the number of contacts between the imidazolium group and glass, causing therefore a larger number of unattached imidazole rings, which could then contribute to the polarity of the films.

On the other hand, the larger sensitivity of the γSp component of PIMb to DI (in comparison with γSp of PIMa) shows that the methylation in the C^+−H group of PIMa has an effect on the adhesion, regardless of the fact that the H-bonds associated with PIMa are considered to have low energies (e.g., less than 17 kJ/mol).[5]

As mentioned before, there is a lack of understanding on the effect of cosolvents on the solution-thermodynamics and drying-kinetics of conjugated molecules, and that for the case of DI, there are no reports available.[31] However, from computational and empirical studies in solution-phase, it is known that DI disrupts the H-bonding structure of water,[37] causing a "coating" effect of groups of DI molecules

https://dx.doi.org/10.1021/acs.langmuir.9b03095
Langmuir 2020, 36, 2278−2290

surrounding the hydrophobic parts of the solutes,[38] probably due to the presence of "clusters" of water and DI being formed at binary 50/50 mixtures.[38,39]

Therefore, the detailed mechanism behind the different effect DI has on PIMa and PIMb during the processing (i.e., deposition of films) involves thermodynamics of solvation in solution and drying kinetics and requires further studies.

CONCLUSIONS

Our results show that methylation of the imidazolium functionality modifies the concentration-driven aggregation, which ends the impact on the surface properties of spin-coated films.

With respect to the films, larger extent of imidazolium-methylation generates smaller values of total SFE, γS, (by around 2 mN/m). This could indicate a larger degree of film ordering in comparison to the polymer with decreased methylation. In optoelectronic devices, such a change in γS would be capable of changing the morphology, miscibility, and segregation between adjacent layers or between layers and electrodes.

Imidazolium-methylation causes a decrease in both the components of γS (γSp and γSd), regardless of the processing solvent. However, the decrease is much larger in γSp, which decreases around 9−14%, whereas γSd decreases only 0.1−2%. This indicates that methylation decreases the polar nature of the imidazolium ring, which could be related to the blocking of the H-bonding donor capabilities in the imidazolium ring, regardless of the fact that the H-bonds associated with PIMa are considered to have low energies (e.g., less than 17 kJ/mol).[5]

The values of γS obtained in the present work are similar to those of doped films of neutral conjugated polymers: the polymer with the smaller extent of imidazolium-methylation (PIMa) shows values of γS similar to doped films of PANI, whereas PIMb shows values of γS similar to doped films of P3HT or PPy. However, the PIMa−PIMb films have a larger predominance of γSd (larger values of the ratio $\gamma Sd/\gamma Sp$) than the films of neutral conjugated polymers. This indicates that the cationic functionalities in PIMa−PIMb (and CPEs in general) contribute in a smaller extent to the surface energy, in comparison with regular dopants in films made of neutral conjugated polymers. This could be explained by the restriction in mobility in the ionic functionalities in a CPE (i.e., attachment to a polymer backbone).

With regard to the effect of DI, its presence slightly increases γSp, especially in the polymer with larger imidazolium-methylation (PIMb). On the other hand, DI causes negligible changes in γSd for both polymers. The CA values of diiodomethane suggest that DI decreases the number of contacts between the imidazolium group and glass, causing therefore a larger number of unattached imidazole rings, which could then contribute to the polarity of the films. Therefore, DI seems to decrease the imidazolium−glass interactions, particularly, for the polymer with larger extent of methylation (and therefore capable of interacting only through electrostatic interactions, see Scheme 2), whereas the polymer with H-bonding donor capabilities is less affected.

EPR results show that the differences in film structuration between the polymers with different methylations originate in the early stages of aggregation. Four different spin probes provide different points of view about the polymer structure with respect to the differently polar and charged regions. The hydrophobic probe (5DSA) better solubilizes in the methylated-PIMb aggregates, indicating higher packing of the hydrophobic region with respect to PIMa aggregates.

In the case of probes with hydrophobic and hydrophilic components (CAT8 and CAT16), in aggregates, their solubilization varies as a function of the extent of imidazolium-methylation. In aggregates, the probe possessing an octyl chain (CAT8) stays at the interface. Therefore, the methyl group of PIMb imidazolium repulses its charged group, whereas better solubility is obtained in the presence of PIMa. Conversely, the probe possessing a hexyldecyl chain (CAT16) is better solubilized by PIMb aggregates. EPR results also show that PIMb aggregates, because of the presence of the methyl group, are more packed in their hydrophobic region than PIMa aggregates. On the contrary, surface packing decreases for PIMb with respect to PIMa, and hence, methyl groups repulse the positively charged groups on the surface.

Finally, the small probe without a hydrophobic chain (TOH) is equivalently solubilized by both polymers, regardless of the extent of imidazolium-methylation, probably due to water competition for H-bonding.

ASSOCIATED CONTENT

Supporting Information

The Supporting Information is available free of charge at https://pubs.acs.org/doi/10.1021/acs.langmuir.9b03095.

CA values of each of the probe liquids (glycerol, ethylene glycol, formamide, and diiodomethane) on plasma-activated glass, plasma-glass spin-coated with water (glass−water), and plasma-glass spin-coated with DI (glass−DI) and plots of the estimated values of the SFE and its dispersive and polar contributions, as estimated using the OWRK and Wu's models, from films of PIMa or PIMb processed from water or W−DI (PDF)

AUTHOR INFORMATION

Corresponding Authors

Sergio E. Domínguez − *Department of Chemistry, Turku University Centre for Materials and Surfaces (MATSURF), University of Turku, 20014 Turku, Finland;* orcid.org/0000-0002-5702-9889; Email: suesdo@utu.fi

Carita Kvarnström − *Department of Chemistry, Turku University Centre for Materials and Surfaces (MATSURF), University of Turku, 20014 Turku, Finland;* orcid.org/0000-0002-8734-2294; Email: carkva@utu.fi

Authors

Antti Vuolle − *Department of Chemistry, Turku University Centre for Materials and Surfaces (MATSURF), University of Turku, 20014 Turku, Finland*

Michela Cangiotti − *Department of Pure and Applied Sciences (DiSPeA), University of Urbino, 61029 Urbino, Italy*

Alberto Fattori − *Department of Pure and Applied Sciences (DiSPeA), University of Urbino, 61029 Urbino, Italy*

Timo Ääritalo − *Department of Chemistry, Turku University Centre for Materials and Surfaces (MATSURF), University of Turku, 20014 Turku, Finland*

Pia Damlin − *Department of Chemistry, Turku University Centre for Materials and Surfaces (MATSURF), University of Turku, 20014 Turku, Finland*

https://dx.doi.org/10.1021/acs.langmuir.9b03095
Langmuir 2020, 36, 2278−2290

M. Francesca Ottaviani − *Department of Pure and Applied Sciences (DiSPeA), University of Urbino, 61029 Urbino, Italy;* orcid.org/0000-0002-4681-4718

Complete contact information is available at: https://pubs.acs.org/10.1021/acs.langmuir.9b03095

Notes

The authors declare no competing financial interest.

■ ACKNOWLEDGMENTS

SED deeply acknowledges the Mexican National Council for Science and Technology (CONACyT) for the international doctoral scholarship no. 310828, the Turku University Foundation (Turun Yliopistosäätiö), the Real estate Foundation (Kiinteistösäätiö), the partial support from the Finnish National Doctoral Programme in Nanoscience (NGS-NANO), and the Doctoral Programme in Physical and Chemical Sciences (PCS) from the University of Turku. M.F.O., M.C., and A.F. thank DiSPeA, University of Urbino, for funding and Dr. Xuegong Lei from Columbia University, NY, USA, for the paramagnetic probes CAT8 and CAT16.

■ REFERENCES

(1) Scherf, U.; Evans, R. C.; Gutacker, A.; Bazan, G. C. All-Conjugated Rod−Rod Diblock Copolymers Containing Conjugated Polyelectrolyte Blocks. In *Conjugated Polyelectrolytes*; John Wiley & Sons, Ltd., 2013; pp 65−89.

(2) Burrows, H. D.; Knaapila, M.; Fonseca, S. M.; Costa, T. Aggregation Properties of Conjugated Polyelectrolytes. In *Conjugated Polyelectrolytes*; John Wiley & Sons, Ltd., 2013; pp 127−167.

(3) Li, H.; Yang, R.; Bazan, G. C. Fluorescence Energy Transfer to Dye-Labeled DNA from a Conjugated Polyelectrolyte Prequenched with a Water-Soluble C60derivative. *Macromolecules* **2008**, *41*, 1531−1536.

(4) Stay, D. P.; Robinson, S. G.; Lonergan, M. C. 3. Development and Applications of Ion-Functionalized Conjugated Polymers. In *Iontronics Ionic Carriers in Organic Electronic Materials and Devices*; CRC Press, 2011.

(5) Matthews, R. P.; Welton, T.; Hunt, P. A. Competitive Pi Interactions and Hydrogen Bonding within Imidazolium Ionic Liquids. *Phys. Chem. Chem. Phys.* **2014**, *16*, 3238−3253.

(6) Hunt, P. A.; Ashworth, C. R.; Matthews, R. P. Hydrogen Bonding in Ionic Liquids. *Chem. Soc. Rev.* **2015**, *44*, 1257−1288.

(7) Matthews, R. P.; Welton, T.; Hunt, P. A. Hydrogen Bonding and $\pi-\pi$ Interactions in Imidazolium-Chloride Ionic Liquid Clusters. *Phys. Chem. Chem. Phys.* **2015**, *17*, 14437−14453.

(8) Wang, Y.-L.; Laaksonen, A.; Fayer, M. D. Hydrogen Bonding versus $\pi-\pi$ Stacking Interactions in Imidazolium−Oxalatoborate Ionic Liquid. *J. Phys. Chem. B* **2017**, *121*, 7173−7179.

(9) Grabowski, S. J. What Is the Covalency of Hydrogen Bonding? *Chem. Rev.* **2011**, *111*, 2597−2625.

(10) Steiner, T. The Hydrogen Bond in the Solid State. *Angew. Chem., Int. Ed.* **2002**, *41*, 48−76.

(11) Houston, J. E.; Richeter, S.; Clément, S.; Evans, R. C. Molecular Design of Interfacial Layers Based on Conjugated Polythiophenes for Polymer and Hybrid Solar Cells. *Polym. Int.* **2017**, *66*, 1333−1348.

(12) Lim, K.-G.; Park, S. M.; Woo, H. Y.; Lee, T.-W. Elucidating the Role of Conjugated Polyelectrolyte Interlayers for High-Efficiency Organic Photovoltaics. *ChemSusChem* **2015**, *8*, 3062−3068.

(13) Kesters, J.; Govaerts, S.; Pirotte, G.; Drijkoningen, J.; Chevrier, M.; Van Den Brande, N.; Liu, X.; Fahlman, M.; Van Mele, B.; Lutsen, L.; et al. High-Permittivity Conjugated Polyelectrolyte Interlayers for High-Performance Bulk Heterojunction Organic Solar Cells. *ACS Appl. Mater. Interfaces* **2016**, *8*, 6309−6314.

(14) Lee, S.; Nguyen, T. L.; Lee, S. Y.; Jang, C. H.; Lee, B. R.; Jung, E. D.; Park, S. Y.; Yoon, Y. J.; Kim, J. Y.; Woo, H. Y.; et al. Conjugated Polyelectrolytes Bearing Various Ion Densities: Spontaneous Dipole Generation, Poling-Induced Dipole Alignment, and Interfacial Energy Barrier Control for Optoelectronic Device Applications. *Adv. Mater.* **2018**, *30*, 1706034.

(15) Lee, W.; Seo, J. H.; Woo, H. Y. Conjugated Polyelectrolytes: A New Class of Semiconducting Material for Organic Electronic Devices. *Polymer* **2013**, *54*, 5104−5121.

(16) Kesters, J.; Ghoos, T.; Penxten, H.; Drijkoningen, J.; Vangerven, T.; Lyons, D. M.; Verreet, B.; Aernouts, T.; Lutsen, L.; Vanderzande, D.; et al. Imidazolium-Substituted Polythiophenes as Efficient Electron Transport Materials Improving Photovoltaic Performance. *Adv. Energy Mater.* **2013**, *3*, 1180−1185.

(17) Seo, J. H.; Gutacker, A.; Sun, Y.; Wu, H.; Huang, F.; Cao, Y.; Scherf, U.; Heeger, A. J.; Bazan, G. C. Improved High-Efficiency Organic Solar Cells via Incorporation of a Conjugated Polyelectrolyte Interlayer. *J. Am. Chem. Soc.* **2011**, *133*, 8416−8419.

(18) Zilberberg, K.; Behrendt, A.; Kraft, M.; Scherf, U.; Riedl, T. Ultrathin Interlayers of a Conjugated Polyelectrolyte for Low Work-Function Cathodes in Efficient Inverted Organic Solar Cells. *Org. Electron.* **2013**, *14*, 951−957.

(19) Wang, K.; Liu, C.; Meng, T.; Yi, C.; Gong, X. Inverted Organic Photovoltaic Cells. *Chem. Soc. Rev.* **2016**, *45*, 2937−2975.

(20) Rider, D. A.; Worfolk, B. J.; Harris, K. D.; Lalany, A.; Shahbazi, K.; Fleischauer, M. D.; Brett, M. J.; Buriak, J. M. Stable Inverted Polymer/Fullerene Solar Cells Using a Cationic Polythiophene Modified PEDOT:PSS Cathodic Interface. *Adv. Funct. Mater.* **2010**, *20*, 2404−2415.

(21) Po, R.; Carbonera, C.; Bernardi, A.; Camaioni, N. The Role of Buffer Layers in Polymer Solar Cells. *Energy Environ. Sci.* **2011**, *4*, 285−310.

(22) Kim, M.; Lee, J.; Jo, S. B.; Sin, D. H.; Ko, H.; Lee, H.; Lee, S. G.; Cho, K. Critical Factors Governing Vertical Phase Separation in Polymer−PCBM Blend Films for Organic Solar Cells. *J. Mater. Chem. A* **2016**, *4*, 15522−15535.

(23) Lee, H. S.; Kim, D. H.; Cho, J. H.; Hwang, M.; Jang, Y.; Cho, K. Effect of the Phase States of Self-Assembled Monolayers on Pentacene Growth and Thin-Film Transistor Characteristics. *J. Am. Chem. Soc.* **2008**, *130*, 10556−10564.

(24) Treat, N. D.; Brady, M. A.; Smith, G.; Toney, M. F.; Kramer, E. J.; Hawker, C. J.; Chabinyc, M. L. Interdiffusion of PCBM and P3HT Reveals Miscibility in a Photovoltaically Active Blend. *Adv. Energy Mater.* **2011**, *1*, 82−89.

(25) Singh, R.; Suranagi, S. R.; Lee, J.; Lee, H.; Kim, M.; Cho, K. Unraveling the Efficiency-Limiting Morphological Issues of the Perylene Diimide-Based Non-Fullerene Organic Solar Cells. *Sci. Rep.* **2018**, *8*, 2849.

(26) Kouijzer, S.; Michels, J. J.; van den Berg, M.; Gevaerts, V. S.; Turbiez, M.; Wienk, M. M.; Janssen, R. A. J. Predicting Morphologies of Solution Processed Polymer:Fullerene Blends. *J. Am. Chem. Soc.* **2013**, *135*, 12057−12067.

(27) Manders, J. R.; Tsang, S.-W.; Hartel, M. J.; Lai, T.-H.; Chen, S.; Amb, C. M.; Reynolds, J. R.; So, F. Solution-Processed Nickel Oxide Hole Transport Layers in High Efficiency Polymer Photovoltaic Cells. *Adv. Funct. Mater.* **2013**, *23*, 2993−3001.

(28) Lee, I.; Noh, J.; Lee, J.-Y.; Kim, T.-S. Cooptimization of Adhesion and Power Conversion Efficiency of Organic Solar Cells by Controlling Surface Energy of Buffer Layers. *ACS Appl. Mater. Interfaces* **2017**, *9*, 37395−37401.

(29) Dupont, S. R.; Voroshazi, E.; Heremans, P.; Dauskardt, R. H. Adhesion Properties of Inverted Polymer Solarcells: Processing and Film Structure Parameters. *Org. Electron.* **2013**, *14*, 1262−1270.

(30) Higgins, M. J.; Wallace, G. G. Surface and Biomolecular Forces of Conducting Polymers. *Polym. Rev.* **2013**, *53*, 506−526.

(31) McDowell, C.; Abdelsamie, M.; Toney, M. F.; Bazan, G. C. Solvent Additives: Key Morphology-Directing Agents for Solution-Processed Organic Solar Cells. *Adv. Mater.* **2018**, *30*, 1707114.

(32) Urbánek, P.; di Martino, A.; Gladyš, S.; Kuřitka, I.; Minařík, A.; Pavlova, E.; Bondarev, D. Polythiophene-Based Conjugated Polyelectrolyte: Optical Properties and Association Behavior in Solution. *Synth. Met.* **2015**, *202*, 16−24.
(33) Domínguez, S. E.; Meriläinen, M.; Ääritalo, T.; Damlin, P.; Kvarnström, C. Effect of Alkoxy-Spacer Length and Solvent on Diluted Solutions of Cationic Isothiouronium Polythiophenes. *RSC Adv.* **2017**, *7*, 7648−7657.
(34) Domínguez, S. E.; Cangiotti, M.; Fattori, A.; Ääritalo, T.; Damlin, P.; Ottaviani, M. F.; Kvarnström, C. Effect of Spacer Length and Solvent on the Concentration-Driven Aggregation of Cationic Hydrogen-Bonding Donor Polythiophenes. *Langmuir* **2018**, *34*, 7364−7378.
(35) Ottaviani, M. F.; Cangiotti, M.; Fiorani, L.; Barnard, A.; Jones, S. P.; Smith, D. K. Probing Dendron Structure and Nanoscale Self-Assembly Using Computer-Aided Analysis of EPR Spectra. *New J. Chem.* **2012**, *36*, 469−476.
(36) Santeusanio, S.; Attanasi, O. A.; Majer, R.; Cangiotti, M.; Fattori, A.; Ottaviani, M. F. Effect of Hydrogenated Cardanol on the Structure of Model Membranes Studied by EPR and NMR. *Langmuir* **2013**, *29*, 11118.
(37) Kris, M. R. Effect of 1,4-Dioxane on the Complexation of Lanthanides with α-Hydroxy-Isobutyrate. Doctor of Philosophy, Department of Chemistry, Washington State University, 2010, No. December.
(38) Burrows, H. D.; Fonseca, S. M.; Silva, C. L.; Pais, A. A. C. C.; Tapia, M. J.; Pradhan, S.; Scherf, U. Aggregation of the Hairy Rod Conjugated Polyelectrolyte Poly{1,4-Phenylene-[9,9-Bis(4-Phenoxybutylsulfonate)]Fluorene-2,7-Diyl} in Aqueous Solution: An Experimental and Molecular Modelling Study. *Phys. Chem. Chem. Phys.* **2008**, *10*, 4420−4428.
(39) Luong, T. Q.; Verma, P. K.; Mitra, R. K.; Havenith, M. Onset of Hydrogen Bonded Collective Network of Water in 1,4-Dioxane. *J. Phys. Chem. A* **2011**, *115*, 14462−14469.
(40) Bhavya, P.; Melavanki, R.; Kusanur, R.; Sharma, K.; Muttannavar, V. T.; Naik, L. R. Effect of Viscosity and Dielectric Constant Variation on Fractional Fluorescence Quenching Analysis of Coumarin Dye in Binary Solvent Mixtures. *Luminescence* **2018**, *33*, 933−940.
(41) Nakagawa, T.; Hatano, J.; Matsuo, Y. Influence of Additives in Bulk Heterojunction Solar Cells Using Magnesium Tetraethynylporphyrin with Triisopropylsilyl and Anthryl Substituents. *J. Porphyrins Phthalocyanines* **2014**, *18*, 735−740.
(42) Chen, S.; Liu, Z.; Ge, Z. Synthesis, Characterization and Photovoltaic Properties of Three New 3,4-Dithienyl-Substituted Polythiophene Derivatives. *Polym. J.* **2016**, *48*, 101−110.
(43) Khan, M. Z. H. Effect of ITO Surface Properties on SAM Modification: A Review toward Biosensor Application. *Cogent Eng.* **2016**, *3*, 1170097.
(44) Khan, M. Z. H.; Nakanishi, T.; Kuroiwa, S.; Hoshi, Y.; Osaka, T. Effect of Surface Roughness and Surface Modification of Indium Tin Oxide Electrode on Its Potential Response to Tryptophan. *Electrochim. Acta* **2011**, *56*, 8657−8661.
(45) Xu, J.; Wang, C.; Tian, Y.; Wu, B.; Wang, S.; Zhang, H. Glass-on-LiNbO3 Heterostructure Formed via a Two-Step Plasma Activated Low-Temperature Direct Bonding Method. *Appl. Surf. Sci.* **2018**, *459*, 621−629.
(46) Viinikanoja, A.; Areva, S.; Kocharova, N.; Ääritalo, T.; Vuorinen, M.; Savunen, A.; Kankare, J.; Lukkari, J. Structure of Self-Assembled Multilayers Prepared from Water-Soluble Polythiophenes. *Langmuir* **2006**, *22*, 6078−6086.
(47) Malika Jeffries-El, R. D. M. 9. Regioregular Polythiophenes. In *Handbook of Conducting Polymers*, 3rd ed.; Terje, A., Skotheim, J. R. R., Eds., Conjugated Polymers Theory, Synthesis, Properties, and Characterization; CRC Press Taylor & Francis Group, 2007.
(48) Budil, D. E.; Lee, S.; Saxena, S.; Freed, J. H. Nonlinear-Least-Squares Analysis of Slow-Motion EPR Spectra in One and Two Dimensions Using a Modified Levenberg-Marquardt Algorithm. *J. Magn. Reson., Ser. A* **1996**, *120*, 155−189.
(49) Belandria, V.; Mohammadi, A. H.; Richon, D. Volumetric Properties of the (Tetrahydrofuran + Water) and (Tetra-n-Butyl Ammonium Bromide + Water) Systems: Experimental Measurements and Correlations. *J. Chem. Thermodyn.* **2009**, *41*, 1382−1386.
(50) Nayak, J. N.; Aralaguppi, M. I.; Kumar Naidu, B. V.; Aminabhavi, T. M. Thermodynamic Properties of Water + Tetrahydrofuran and Water + 1,4-Dioxane Mixtures at (303.15, 313.15, and 323.15) K. *J. Chem. Eng. Data* **2004**, *49*, 468−474.
(51) Critchfield, F. E.; Gibson, J. A., Jr.; Hall, J. L. Dielectric Constant for the Dioxane-Water System from 20 to 35°. *J. Am. Chem. Soc.* **1953**, *75*, 1991−1992.
(52) Omota, L.-M.; Iulian, O.; Omota, F.; Ciocirlan, O. Densities and Derived Properties of Water, 1,4-Dioxane and Dimethyl Sulfoxide Binary and Ternary Systems at Temperatures from 293.15 K to 313.15 K. *Rev. Roum. Chim.* **2009**, *54*, 63−73.
(53) Barton, A. F. M. *CRC Handbook of Solubility Parameters and Other Cohesion Parameters*, 2nd ed.; Barton, A. F. M., Ed.; CRC Press, 1991.
(54) Hansen, C. M. *Hansen Solubility Parameters: A User's Handbook*, 2nd ed.; Hansen, C. M., Ed.; CRC Press, 2007.
(55) Dalstein, L.; Potapova, E.; Tyrode, E. The Elusive Silica/Water Interface: Isolated Silanols under Water as Revealed by Vibrational Sum Frequency Spectroscopy. *Phys. Chem. Chem. Phys.* **2017**, *19*, 10343−10349.
(56) Zhuravlev, L. T. Concentration of Hydroxyl Groups on the Surface of Amorphous Silicas. *Langmuir* **1987**, *3*, 316−318.
(57) Pouryousefy, E.; Xie, Q.; Saeedi, A. Effect of Multi-Component Ions Exchange on Low Salinity EOR: Coupled Geochemical Simulation Study. *Petroleum* **2016**, *2*, 215−224.
(58) Matisons, J. G. Silanes and Siloxanes as Coupling Agents to Glass: A Perspective. In *Silicone Surface Science*; Owen, M. J., Dvornic, P. R., Eds.; Advances in Silicon Science; Springer Netherlands: Dordrecht, 2012; pp 281−298.
(59) Wu, J.; Liu, F.; Yang, H.; Xu, S.; Xie, Q.; Zhang, M.; Chen, T.; Hu, G.; Wang, J. Effect of Specific Functional Groups on Oil Adhesion from Mica Substrate: Implications for Low Salinity Effect. *J. Ind. Eng. Chem.* **2017**, *56*, 342−349.
(60) Schuster, J. M.; Schvezov, C. E.; Rosenberger, M. R. Analysis of the Results of Surface Free Energy Measurement of Ti6Al4V by Different Methods. *Procedia Mater. Sci.* **2015**, *8*, 732−741.
(61) Thomsen, F. KRUSS Technical Note TN315e. *Custom-Made Models: From Contact Angle to Surface Free Energy*, December 2008.
(62) Shigematsu, M.; Morita, M.; Sakata, I.; Sugihara, G. Phase Separation State in Hemicellulose and Lignin Blends Analyzed by Contact Angle Measurements. *Macromol. Chem. Phys.* **1996**, *197*, 177−183.
(63) Liu, M. J.; Tzou, K.; Gregory, R. V. Influence of the Doping Conditions on the Surface Energies of Conducting Polymers. *Synth. Met.* **1994**, *63*, 67−71.
(64) Tsai, Y.-T.; Choi, C.-H.; Gao, N.; Yang, E.-H. Tunable Wetting Mechanism of Polypyrrole Surfaces and Low-Voltage Droplet Manipulation via Redox. *Langmuir* **2011**, *27*, 4249−4256.
(65) Li, A.-F.; Wang, J.-H.; Wang, F.; Jiang, Y.-B. Anion Complexation and Sensing Using Modified Urea and Thiourea-Based Receptors. *Chem. Soc. Rev.* **2010**, *39*, 3729.
(66) Fan, E.; Van Arman, S. A.; Kincaid, S.; Hamilton, A. D. Molecular Recognition: Hydrogen-Bonding Receptors That Function in Highly Competitive Solvents. *J. Am. Chem. Soc.* **1993**, *115*, 369−370.
(67) Dormidontova, E. E. Role of Competitive PEO−Water and Water−Water Hydrogen Bonding in Aqueous Solution PEO Behavior. *Macromolecules* **2002**, *35*, 987−1001.
(68) Rymuszka, D.; Terpiłowski, K.; Hołysz, L. Influence of Volume Drop on Surface Free Energy of Glass. *Ann. UMCS, Chem.* **2014**, *68*, 121−132.
(69) Jańczuk, B.; Choma, I.; Dawidowicz, A. L.; Kliszcz, A.; Białopiotrowicz, T. Correlation between the Surface Free Energy of Modified and Non-Modified Glasses with Controlled Porosity and Their Sorption Properties. *Chromatographia* **1990**, *30*, 382−387.

https://dx.doi.org/10.1021/acs.langmuir.9b03095
Langmuir 2020, 36, 2278−2290

(70) Yan, R.; Wang, Y.; Duncan, T. V.; Shieh, Y. C. Effect of Polymer and Glass Physicochemical Properties on MS2 Recovery from Food Contact Surfaces. *Food Microbiol.* **2020**, *87*, 103354.

https://dx.doi.org/10.1021/acs.langmuir.9b03095
Langmuir 2020, 36, 2278−2290